The current issue and full text archive of this journal is available at
www.emeraldinsight.com/0961-5539.htm

Finite volume method for the solution of flow on distorted meshes

D. McBride, N. Croft and M. Cross
School of Engineering, University of Wales, Swansea, Wales, UK

Abstract

Purpose – To improve flow solutions on meshes with cells/elements which are distorted/non-orthogonal.

Design/methodology/approach – The cell-centred finite volume (FV) discretisation method is well established in computational fluid dynamics analysis for modelling physical processes and is typically employed in most commercial tools. This method is computationally efficient, but its accuracy and convergence behaviour may be compromised on meshes which feature cells with non-orthogonal shapes, as can occur when modelling very complex geometries. A co-located vertex-based (VB) discretisation and partially staggered, VB/cell-centred (CC), discretisation of the hydrodynamic variables are investigated and compared with purely CC solutions on a number of increasingly distorted meshes.

Findings – The co-located CC method fails to produce solutions on all the distorted meshes investigated. Although more expensive computationally, the co-located VB simulation results always converge whilst its accuracy appears to grace-fully degrade on all meshes, no matter how extreme the element distortion. Although the hybrid, partially staggered, formulations also allow solutions on all the meshes, the results have larger errors than the co-located vertex based method and are as expensive computationally; thus, offering no obvious advantage.

Research limitations/implications – Employing the ability of the VB technique to resolve the flow field on a distorted mesh may well enable solutions to be obtained on complex meshes where established CC approaches fail

Originality/value – This paper investigates a range of cell centred, vertex based and hybrid approaches to FV discretisation of the NS hydrodynamic variables, in an effort characterize their capability at generating solutions on meshes with distorted or non-orthogonal cells/elements.

Keywords Meshes, Flow, Fluid dynamics

Paper type Research paper

1. Introduction

Computational fluid dynamics (CFD) modelling of "real-life" processes requires a mesh that accurately represents the true geometry of the physical domain. This often means fitting a mesh to a highly complex geometry. Of course, fitting a highly orthogonal mesh to a "real-life" geometry can be one of the most time consuming aspects of the CFD modelling process. A mesh that truly represents the physical domain of such a process may well contain regions, aspects of which are badly distorted. Much research has been done in developing mesh generation algorithms to improve the quality and reduce the non-orthogonality of such meshes, see for example Bijl *et al.* (2005) and Chand (2005). However, in many modelling scenarios involving different physical phenomena, such as close coupling between flow and stress, even if a highly orthogonal mesh can represent the initial physical domain, mesh distortion can occur during the solution process. In such multi-physics problems, even if one starts with a

International Journal of Numerical Methods for Heat & Fluid Flow
Vol. 17 No. 2, 2007
pp. 213-239

0961-5539
DOI 10.1108/09615530710723975

high quality mesh it may degrade during the solution process. In such modelling scenarios, a numerical solution technique is required that is robust on unstructured meshes which feature elements with non-orthogonal shapes.

The most frequently used unstructured mesh discretisation methods are the finite element method (FEM) (Zienkiewicz and Morgan, 1983) and the finite volume method (FVM) (Barth, 1992). The finite volume (FV) discretisation technique is well established in CFD analysis. The physically meaningful FV principles of applying conservation laws locally to control volumes has lead to the FV method being the preferred method for modelling physical processes involving the solution of flow. There are a number of FV approaches, usually either vertex-centered, where the unknowns are defined at the mesh nodes or cell-centred (CC), where the unknowns are defined at the element centroid. The most widely used is the CC approach, which is employed in many CFD codes (e.g. CFX (www.ansys.com), FLUENT (www.fluent.com), STAR-CD (www.cd-adapco.com) and PHYSICA (www.multi-physics.com)). This technique is computationally efficient, on a highly orthogonal mesh, using simple approximations to discretise the terms in the transport equation, it has low memory requirements and fast simulation times. However, the method is not robust on an unstructured non-orthogonal mesh and computation of the fluxes is problematic on a non-orthogonal grid. Various discretisation techniques have been developed for unstructured meshes including, edge-based schemes that employ dual control volumes and edge-based data structures (Barth, 1992; Lyra *et al.*, 1994; Crumpton and Giles, 1995; Sorensen *et al.*, 1999) as well as others (Coirier, 1994; Mavriplis, 1995; Haselbacher and Blasek, 2000) who use cell based gradient reconstruction (Jameson *et al.*, 1986) who used cell vertex techniques (Chakrabartty, 1990) who employed a vertex-centred scheme for flow past complex geometries (Boivin *et al.*, 2000; Perron *et al.*, 2004) and who stored solved variables at the cell-circumcenters to enable solutions on unstructured meshes.

Difficulties can occur when approximating the control volume face derivatives, using the standard linear central differencing schemes, employed in most FV codes. Standard schemes are only sufficient if the points involved in calculating control volume face values are connected by a straight line, which is normal to the boundary face, as is the case on an orthogonal mesh. On complex grids, this is not usually the case and the accuracy of the scheme deteriates in areas of poor quality. Corrections have to be made to the usual discretisation process to account for non-orthogonality in the mesh (Croft *et al.*, 1995; Croft, 1998). On distorted grids these corrections are only first-order accurate. Local errors appear in the solution dependant on the extent of mesh distortion and the solution may diverge. Peric (1985) investigated this effect on distorted meshes and proposed grid refinement and smoothing to reduce the error. Moulinec and Wesseling (2000) investigated several different interpolation schemes to improve the derivatives at the cell faces on distorted meshes. Other authors (Barth and Jespersen, 1989; Weiss *et al.*, 1999) proposed different interpolation schemes based on Taylor series expansions. Lehnhauser and Schafe (2002) reported significantly improved accuracy with a multi-dimensional Taylor series expansion scheme which ensured second-order accuracy even on strongly distorted meshes. The problems encountered in discretising the transport equations on distorted meshes are exacerbated when employing pressure-correction schemes in the solution of the incompressible Navier-Stokes equations. Addition of the non-orthogonal correction

terms in the pressure-correction equation is expensive and complex and it is common practice to omit these terms (Demirdzic, 1982; Braaten and Shyy, 1986). However, omission or simplification of these terms can introduce stability problems into the solution process and lead to difficulties with convergence on highly distorted meshes. Since, in complex geometries it is often not possible to have a good quality mesh over the entire domain, many authors have sought to address this problem (Peric, 1990; Cho and Chung, 1994; Lehnhauser and Schafe, 2003; Zhu *et al.*, 2004).

An alternative FV technique is the control volume-FEM, developed by Prakash and Patankar (1985) and described by Baliga (1996) which has successfully been applied to complex flow problems with irregular geometries (Reyes *et al.*, 2001). This method can be viewed in a FV context as a vertex-based FVM (VB) (Taylor *et al.*, 2003). The local variation of a variable within an element is described by simple piecewise polynomial functions allowing distorted meshes to be handled with relative ease. This flexibility of applying the VB discretisation technique to arbitrary irregular meshes is appealing. However, the method requires extensive storage/topological information and the computational cost is far more expensive than the CC technique. Combining aspects of both the FEM and FVM has become increasingly popular and has been applied in a number of research areas. A mixed FEM-FVM, originally developed by Dervieux (1985) has been employed by many in the simulation of turbulent flow, including 3D turbulent compressible flow (Hallo *et al.*, 1997) and large Eddy simulations (Koobus and Farhat, 2004). This method uses finite element discretisation for the diffusive part of the Navier-Stokes equations and FV computations for all other terms. Durlofsky (1993) combined FV-finite elements in the solution of multiphase flow in porous media. Here the fluid pressure field is discretised using finite elements and the fluid phases are computed using the FVM. This method has been applied by Mazzia and Putti (2005) and Chavent *et al.* (2003) amongst others. Hybrid FV-FE have also been employed for viscoelastic flows (Wapperom and Webster, 1998). Here, the FEM is applied to the continuity and momentum equations and the FVM to the constitutive equations for stress. Chan and Kallinderis (1998) used a FV formulation for the 3D Navier-Stokes equations of incompressible flow and a finite element discretisation of the pressure-correction equation. In the fore going methods, although not an exhaustive list, the cell-vertex FVM has commonly been employed on triangle-tetrahedral meshes. The variables are all stored at the same locations, the mesh vertices. In a tetrahedral mesh, there are less vertices than elements, but on a hexahedral mesh there are more vertices than elements and a CC formulation would require less storage.

This paper is an introduction to a study investigating the resolution of flow variables on unstructured skewed meshes whilst working within the FV methodology. As part of this investigation the VB discretisation technique, utilizing element based piecewise linear shape functions, is compared with the CC discretisation method. In this initial study hybrid VB/CC solution methods are investigated in an effort to capture the efficiency of the CC method, whilst retaining the geometric flexibility of the VB discretisation procedure. The paper outlines both the CC and VB approach in the solution of the incompressible Navier-Stokes equations and utilises hybrid discretisation in the solution of partially staggered flow variables. Problems of velocity-pressure coupling and avoiding checkerboard pressure fields are discussed. In the final section, the CC, VB and hybrid schemes are compared on a lid-driven cavity problem. Comparisons are made with benchmark solutions on meshes with different

degrees of skewness. The aim of this paper is to access their ability to improve numerical solution accuracy on distorted meshes. A further paper will detail a combined CC/VB technique which enables well established CC physical models to be employed on meshes of bad quality.

2. The discretisation method

An outline of the discretisation techniques employed in this paper are given in the following sections. Figure 1 shows the control volumes employed in the discretisation process for a 2D mesh.

2.1 Cell-centred approach

In the CC approach, the general variable ϕ is solved and stored at the cell centre (element centroid). The terms in the general transport equation are discretised using finite-difference type approximations to describe how ϕ varies between solution points. These approximations assume that adjacent element centre points lie on a line, perpendicular to the element face, that passes through the face centroid. However, fitting a mesh to a complex geometry frequently leads to some degree of non-orthogonality in the generated mesh requiring corrections to be made to the usual discretisation process. The inclusion of these correction terms allow solutions on meshes with some degree of skewness. However, difficulties arise in calculating the correction terms to any more than first order accuracy. Problems are also encountered as the corrections are functions of the solved variable which can lead to stability problems. Therefore, inclusion of these corrections often leads to oscillatory results, difficulties in convergence and longer simulation times. On highly skewed meshes a high percentage of the solution can comprise of these correction terms and the solution may diverge. A detailed description of the particular discretisation technique used here is given by Croft (1998).

2.2 Vertex-based approach

The VB control volume consists of a number of sub-control volumes constructed around the mesh vertices. A mesh element is divided into a number of sub-control volumes by lines connecting the mid-face and element centre. The surfaces of the sub-control volumes within a mesh element define the control volume surrounding the mesh vertex, as shown in Figure 1 for a 2D mesh. The general variable ϕ is solved and

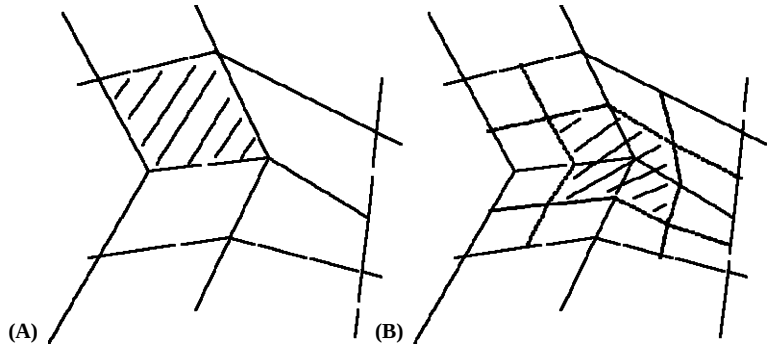

Figure 1.
(a) Cell-centred control volume; (b) vertex-based control volume

stored at the vertices of the mesh elements. The terms in the conservation equation are approximated working in local co-ordinates. This allows for all elements of a certain type to be treated identically regardless of how distorted any element may be in terms of global co-ordinates. The integration points are located at the centre of the sub-control faces which form the control volume boundary. The terms in the general transport equation are discretised using simple linear shape function approximations:

$$\begin{aligned} x(s,t,u) &= \sum_{i=1}^{n} N_i(s,t,u)x_i \\ y(s,t,u) &= \sum_{i=1}^{n} N_i(s,t,u)y_i \\ z(s,t,u) &= \sum_{i=1}^{n} N_i(s,t,u)z_i \end{aligned} \tag{1}$$

where x_i, y_i and z_i are the global co-ordinates at node i and n is the number of nodes associated with the element under consideration:

$$\phi(s,t,u) = \sum_{i=1}^{n} N_i(s,t,u)\phi_i \tag{2}$$

where ϕi is the variable described at node i.

The local co-ordinate system, integration points, shape functions and local to global transformations are given in McBride (2003) along with a detailed description of the discretisation technique.

3. Solution of fluid flow

The momentum transport equations can be written as:

$$\frac{\partial(\rho u_i)}{\partial t} + \mathrm{div}(\rho \underline{u} u_i) - \mathrm{div}(\mu \nabla u_i) = S_{u_i} - \nabla_{x_i} p \tag{3}$$

The velocity field must also satisfy mass conservation:

$$\frac{\partial \rho}{\partial t} + \mathrm{div}(\rho \underline{u}) = S_m \tag{4}$$

For the incompressible Navier-Stokes equations difficulty arises from how to resolve the role played by pressure. A pressure gradient source term appears in all three momentum equations but there is no other equation linked to pressure. A pressure equation can be derived from the continuity equation by expressing velocity derivatives as a function of the pressure gradient using the momentum equations. The most common approach to solving this system of equations, which is employed in this investigation, is a segregated solution procedure, the equations are solved independently by means of an iterative guess and correct strategy, such as the SIMPLE or SIMPLER algorithm (Patankar and Spalding, 1972). However, these methods require some form of under-relaxation to ensure convergence. An alternative

approach, which has been investigated for laminar flow by Ammara and Masson (2004) is to use a fully coupled system, where the pressure-velocity coupling is treated implicitly and momentum, pressure and pseudo-velocity equations are derived and solved simultaneously. This method required no under-relaxation and is reported for laminar Navier-Stokes equation to improve robustness and efficiency.

As a starting point for the solution procedure, the system of algebraic equations obtained from the discretised momentum equations can be expressed in the following form:

$$a_{u_i} u_i - \sum a_{\mathrm{nb}} u_{\mathrm{nb}} = b_{u_i} - \nabla_{x_i} p \tag{5}$$

The velocity field is also subject to the constraint that it must satisfy the continuity equation (4). The discretised form of the continuity equation for a control volume (cv) is:

$$\frac{\rho_{\mathrm{cv}} V_{\mathrm{cv}} - \rho^0_{\mathrm{cv}} V^0_{\mathrm{cv}}}{\Delta t} + \sum_f \rho_f A_f (\underline{u}.\underline{n}) f = V_{\mathrm{cv}} (S_m)_{\mathrm{cv}} \tag{6}$$

Pressure and velocity are intrinsically coupled, if the correct pressure field is applied in the momentum equations the resulting velocity field will satisfy the continuity equation.

3.1 Pressure-velocity coupling

It is well known that co-located discretisation methods that solve and store pressure and velocity components at the same locations can suffer from oscillating (checker-board) pressure predictions. However, in any discretisation technique, if a checker-board pressure field can be supported by both the discretised form of the momentum and continuity equations spurious oscillating pressure predictions can emerge.

In order to prevent checkerboarding in the final solution, the discretisation technique used in the momentum or continuity equation must provide a filter to remove oscillating results. Checkerboarding is overcome by devising interpolation procedures which express face velocities in terms of adjacent pressure values rather than alternate pressure values. The procedure, known as momentum interpolation, does not use pure linear interpolation to define the face velocity. An additional term is included which is dependent on adjacent pressure values. Several variations of this scheme have been proposed (Hsu, 1981; Rhie and Chow, 1983; Peric, 1985; Burns and Wikkles, 1987) but the basic idea remains the same. It is these newly defined face velocity values that are used in the discretision of the continuity equation. Thus, at convergence, it is the face velocities that directly satisfy continuity. The CC velocities only comply with conservation indirectly in that they fulfil the momentum interpolation formula. Another method, which essentially uses the same key idea, is to define a new face velocity field which is driven by the pressure difference between adjacent cell values (Prakash and Patankar, 1985). This new face velocity field can be considered as a type of staggered velocity field. Instead of deriving this velocity field directly, a pseudo velocity field which contains the convection, diffusion and source term, is obtained from the momentum equations, and a pressure gradient term added.

The basic idea behind these interpolation techniques is the replacement of the pressure gradient term, which is obtained using linear interpolation of cell velocities, with a new pressure gradient term which is calculated from adjacent pressure values. The face velocities can now be written in terms of adjacent pressure values and it is these that are used to satisfy continuity. Thus, a checkerboard pressure field would be recognised by these face velocities. Although the momentum equations still contain a pressure gradient term that does not recognise a checkerboard pressure field, such a field would not satisfy the continuity equation.

3.2 Cell-centred solution procedure

The CC solution method employed here utilizes the Rhie and Chow (1983) interpolation method, to avoid spurious pressure predictions and a SIMPLE-type iterative solution technique.

The momentum equations are discretised using Rhie-Chow interpolation to obtain the face velocity components. The control volume pressure gradient, which enters the momentum equations as a source term, is evaluated as a sum of surface integrals over each face bounding the control volume:

$$\int_{\mathrm{cv}} \nabla_{x_i} p dV \simeq \sum_f A_f (n_{x_i})_f p_f \tag{7}$$

where p_f is interpolated from adjacent values.

The pressure-correction procedure employs the SIMPLE algorithm. Initially, the discretised momentum equations are solved using a guessed pressure field (p^*) to yield velocity components u^*, v^* and w^*. A correction term p' is defined as the difference between the correct pressure field p and the guessed pressure field p^*. Similarly velocity correction terms u_i' are defined to relate u_i^* to the correct velocities u_i.

Using the SIMPLE approximation, a face velocity correction term is obtained:

$$(u_i')_f = -\frac{1}{(a_{u_i})_f}(\nabla_{x_i} p')_f \quad = \frac{1}{(a_{u_i})_f} A_f (n_{x_i})_f (p'_P - p'_A) \tag{8}$$

where subscript P indicates the value at the center of the control volume and subscript A indicates the adjacent control volume.

The discretised continuity equation (6), can now be written as:

$$\sum_f \rho_f \frac{A_f^2 n_i^2}{a_i} (p'_P - p'_A)_f = \frac{\rho_P^0 V_P^0 - \rho_P V_P}{\Delta t} - \sum_f A_f \rho_f (\underline{u}^* \cdot \underline{n})_f \tag{9}$$

where $(u_i^*)_f$ is obtained using Rhie-Chow interpolation and the subscript i in the first term indicates a summation over the three coordinate directions.

The above equation leads to a set of linear equations with weak diagonal dominance and can be written in the form:

$$a_P p'_P + \sum_{\mathrm{nb}} a_{\mathrm{nb}} p'_{\mathrm{nb}} = b_P \tag{10}$$

Once the above equation has been solved and a pressure correction field obtained, the pressure field is updated. The SIMPLE approximation tends to lead to an

over-estimation of the pressure correction values, making the pressure-correction equation susceptible to divergence unless some under-relaxation is used during the iterative procedure. In the procedure used here, a relaxation value of 0.6 is set as standard.

It is the element cell values that are updated rather than face values. The velocity correction values are obtained from pressure correction values using the SIMPLE approximation:

$$u_i' = \frac{-\nabla_{x_i} p'}{a_{u_i}} \tag{11}$$

Expanding this equation gives the velocity corrections in terms of pressure corrections in the element and all its neighbours:

$$(u_i')_P = -\frac{1}{(a_{u_i})_P} \sum_f n_{x_i} A_f (\alpha p'_P + (1-\alpha) p'_A) \tag{12}$$

where α is a wieghting factor.

3.3 Vertex-based solution procedure

The VB procedure employs the method of Prakash and Patankar (1985) which defines a new face velocity field which is dependant on adjacent pressure values, to overcome spurious pressure predictions and the revised SIMPLER iterative solution technique.

To initiate the solution procedure the momentum equations are discretised using the VB technique and the velocities (u^i) are stored at the mesh vertices. Initially, the face velocity is obtained employing the shape function interpolation functions:

$$(u^i)_f = \sum_{j=1}^{n} N_j (u^i)_j \tag{13}$$

where n is the number of nodes of the element that bounds the face, j is the element node, and N_j are the interpolation functions.

The control volume pressure gradient can be evaluated as equation (7) or as a sum of sub-volume integrals:

$$\int_{\mathrm{cv}} \nabla_{x_i} p = \sum_{\mathrm{scv}} V_{\mathrm{scv}} \sum_{j=1}^{n} \frac{\partial N_j}{\partial x_i} p_j \tag{14}$$

Once an initial velocity field has been obtained, a pseudo velocity field ($\hat{\underline{u}}, \hat{\underline{v}}$ and $\hat{\underline{w}}$) is defined that does not depend directly on the pressure distribution, using equation (5) and the SIMPLER approximations:

$$\hat{u}_i = \frac{\sum a_{\mathrm{nb}} u_{\mathrm{nb}} + b_{u_i}}{a_{u_i}} \tag{15}$$

$$d^{u_i} = \frac{V}{a_{u_i}} \tag{16}$$

giving:

$$(\hat{u}_i)_{\mathrm{cv}} = (u_i)_{\mathrm{cv}} + (d^{u_i})_{\mathrm{cv}} \left(\frac{\partial p}{\partial x_i}\right)_{\mathrm{cv}} \tag{17}$$

Using conservation principles for the control volume face, a new velocity field ($\tilde{\underline{u}}, \tilde{\underline{v}}$ and $\tilde{\underline{w}}$)can now be defined that is dependent upon adjacent pressure values:

$$(\tilde{u}_i)_f = (\hat{u}_i)_f - (d^{u_i})_f \left(\frac{\partial p}{\partial x_i}\right)_f \tag{18}$$

where $(\hat{u}_i)_f$ and $(d^{u_i})_f$are calculated from nodal values assuming linear variation within an element. The pressure gradient across a face is obtained using local element shape function derivatives:

$$\frac{\partial p}{\partial x_i} = \sum_{j=1}^{n} \frac{\partial N_j}{\partial x_i} p_j \tag{19}$$

where n is the number of nodes belonging to an element and N_j is the shape function associated with node j of the element (which bounds the face). The face pseudo velocity $(\hat{u}^i)_f$ and pressure gradient coefficient $(d^{u_i})_f$ are interpolated linearly from nodal values.

The continuity equation (4) is discretised using the $\tilde{\underline{u}}$ field as follows:

$$\frac{\rho_{\mathrm{cv}} V_{\mathrm{cv}} - \rho^0_{\mathrm{cv}} V^0_{\mathrm{cv}}}{\Delta t} + \sum_f \rho_f A_f (\tilde{\underline{u}} \cdot \underline{n})_f = V_{\mathrm{cv}} (S_m)_{\mathrm{cv}} \tag{20}$$

Substituting equation (18) into equation (20) and rearranging gives:

$$\begin{aligned} \sum_f \sum_{j=1}^{n} \sum_{i=x,y,z} \rho_f A_f d_f^{u_i} \left(\frac{\partial N_j}{\partial x_i} \cdot n_i\right) p_j = \sum_{\mathrm{scv}} \frac{\rho^0_{\mathrm{scv}} V^0_{\mathrm{scv}} - \rho_{\mathrm{scv}} V_{\mathrm{scv}}}{\Delta t} \\ - \sum_f A_f \rho_f (\hat{\underline{u}} \cdot \underline{n})_f + V_{\mathrm{cv}} (S_m)_{\mathrm{cv}} \end{aligned} \tag{21}$$

For Dirichlet boundary conditions, where velocity is specified, the known mass flux is transferred to the right-hand side of equation (21) and the corresponding pressure coefficient d^{u_i} is set to zero. If pressure is known at the boundary node, the control volume cofficient is set equal to one, all off-diagonal terms are set to zero and the right-hand side set equal to the known pressure. At outflows where pressure and velocity are not known, equation (21) is completed by estimating the mass flux out of the domain based on the most recently calculated values of the velocity field at the boundary.

This leads to a positive definite system of linear equations with a larger bandwidth than the CC approach. For a hexahedral mesh there are a possible 27 non-zero coefficients, compared to seven in the CC case. The pressure equations can be transformed into a system of pressure-correction equations using:

$$[A][p'] = [b'], \quad \text{where } [b'] = [\hat{b}] - [A][p^*] \tag{22}$$

No relaxation is applied to pressure, otherwise the resulting corrected $\tilde{\underline{u}}$ field will not satisfy mass conservation. The $\tilde{u}_i$ velocities are updated using equation (18) with no relaxation. It is this mass conserving face velocity field that is used in the discretised momentum equations. In order to advance the solution process, the nodal velocities are also updated using:

$$u_i = \hat{u}_i - d^{u_i} \frac{\partial p}{\partial x_i} \tag{23}$$

a relaxation factor of 0.7 is applied as standard.

4. Hybrid discretisation of hydrodynamic variables

This section outlines hybrid discretisation solutions for the hydrodynamic variables, pressure and velocity. It will be demonstrated later that the CC discretisation method is fast and efficient, but does not handle skewed meshes with the ease of the VB technique. The question is, is there a method that can combine the efficiency of the CC technique whilst retaining the geometric flexibility of the VB technique?

The pressure field could be obtained using the VB discretisation procedure whilst using CC discretisation for the momentum equations. Obtaining better resolution of the pressure field on distorted meshes should give improved resolution of the velocity field since pressure is the driving force for the components of velocity. The solution of the momentum equations is used as a vehicle for advancing the solution process. The velocity components are updated and defined in terms of local pressure gradients. Using the momentum equations to obtain a pseudo velocity field but defining a face velocity field using VB techniques allows for better definition of the local pressure gradient (from eight points on a hexahedral element) on a distorted mesh.

Conversely, the VB technique, which has the ability to handle distorted meshes, could be used to discretise the momentum equations. Would the velocity field obtained from the discretised momentum equations be sufficient to couple with CC techniques for the pressure field? The face velocity components would now be defined in terms of the pressure difference across an element face (from two points on a hexahedral mesh). Would this weaker definition of the pressure gradient term effect the final solution on distorted meshes?

In both scenarios, mass is conserved over the scalar control volume not the momentum control volume. Unlike unstructured staggered grid procedures, the VB and CC control volume face integration points do not coincide, obtaining values at the location required involves interpolation. Estimating VB values from CC values and vice-versa could potentially introduce errors into the solution procedure.

As in co-located formulations, the hybrid discretisation has the potential for decoupling to occur and checkerboard pressure fields to emerge. Velocity and pressure are only partially staggered. The velocity components are located at the corners of the pressure control volume and vice versa. A checkerboard pressure field would give a zero pressure gradient term. The discretised momentum equations would not recognise a checkerboard pressure field. Conversely, using linear interpolation to obtain face velocity values would result in a checkerboard velocity field satisfying the continuity equation. In order to prevent spurious pressure predictions the hybrid discretisation of the continuity equation defines a face velocity field which is dependant on adjacent pressure values. Thus, solution of the continuity equation does not allow checkerboard pressure values to emerge.

A detailed account of the hybrid discretisation and solution procedure is given in the following sections.

4.1 Pressure – vertex-based, velocity – cell-centred

The pressure field is obtained using VB techniques, where pressure is solved and stored at the mesh vertices. The velocity field is obtained using CC techniques where the velocity components are solved and stored at the element center. As a starting point, the momentum equations are discretised using CC techniques. The inclusion of the non-orthogonal correction terms in the discretised momentum equations leads to stability and convergence problems, therefore these terms were omitted. The element cell pressure gradient, which enters the momentum equation as a source term, is calculated from nodal values using local shape function derivatives:

$$\frac{\partial p}{\partial x_i} = \sum_{j=1}^{n} \frac{\partial N_j}{\partial x_i} p_j \tag{24}$$

The momentum equations are solved and components of velocity are obtained at the element centroid. Pseudo velocity components $\hat{u}_e, \hat{v}_e, \hat{w}_e$ and pressure gradient cofficients d_e^u, d_e^v, d_e^w are defined for each element, as in equations (15) and (16).

A new face velocity field $\tilde{u}_f$, dependant on adjacent pressure values, is defined on the face of the VB control volume:

$$(\tilde{u}_i)_f = (\hat{u}_i)_f - (d^{u_i})_f \left(\frac{\partial p}{\partial x_i}\right)_f \tag{25}$$

The above equation requires the sub-control volume face values to be defined for the pseudo velocity, pressure gradient coefficient and pressure gradient terms. Since, pressure values are located at the mesh nodes, the face pressure gradients can easily be calculated using the derivatives of the interpolation functions, as shown in equation (19).

What is not so obvious is how to obtain VB sub-control volume face values from the element based pseudo velocities and pressure gradient coefficients. To illustrate this, Figure 2 shows a 2D mesh element containing faces of the VB sub-control volumes. Assuming element centre values are known but values, ϕ_{scv}, are required at sub-control volume face integration points. If, for example, the mesh element shown contains a local maximum value, $\phi_{ele} = 4$, and all surrounding elements have values of

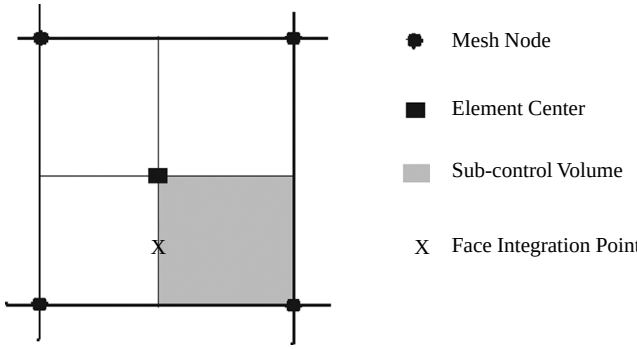

Figure 2.
Element containing VB control volume face

$\phi_{nbr} = 3$, assuming equal distances and linear variation, interpolating from element centre values would give $\phi_{scv} = 3.75$. However, if the mesh was distorted the sub-control volume face integration point would no longer lie on the line connecting adjacent element centre points and a correction term would be required. If nodal values are obtained from element values, local linear shape functions can be employed to obtain VB face values. On a structured mesh simple averaging of element values can easily approximate nodal values. On unstructured meshes, the distance from the element centre to the mesh node needs to be taken into account as follows:

$$\phi_{node} = \frac{\sum_{i=1}^{ne}(\phi d^{-1})}{\sum_{i=1}^{ne} d^{-1}} \tag{26}$$

where d is the distance from the element centre to the mesh node and ne is the number of elements associated with the node. In both cases, extrapolation errors may occur at the boundary.

Using weighted averaging to obtain nodal values and employing shape functions to obtain face values, introduces the potential for local minima and maxima values to be lost. Referring to Figure 2 and assuming $\phi_{ele} = 4$ and $\phi_{nbr} = 3$ the interpolated nodal values ϕ_{node} for the element would be $\phi_{node} = 3.25$ giving $\phi_{scv} = 3.25$ which is incorrect. An improved estimate can be obtained by including the element centre value when evaluating ϕ_{scv}. The element centroid forms a corner point of each face. If all other corner points are interpolated from nodal values. The VB face value can then be evaluated from its corner values, which includes the element centroid, in this case giving $\phi_{scv} = 3.625$ which is much closer to $\phi_{scv} = 3.75$.

Once VB face values have been obtained, the VB form of the discretised continuity equation (21) can be transformed into a pressure-correction equation, following VB procedures to obtain nodal pressure values. The mass conserving velocity field is the $\tilde{\underline{u}}$ field and all other transport equations should be discretised over the VB control volume. The momentum equations are only used as a means of advancing the solution of $\tilde{\underline{u}}$. The element based velocity $\underline{u}$ is updated using equation (23) as:

$$(u_i)_e = (\hat{u}_i)_e - (d^{u_i})_e \left(\frac{\partial p}{\partial x_i}\right)_e \tag{27}$$

where the element pressure gradient is evaluated from nodal values using equation (24).

4.2 Pressure – cell-centred, velocity – vertex-based

Here the pressure field is solved and stored at the element centroid and the velocity component, u_i, are solved and stored at the mesh vertices. An initial velocity field is obtained by discretising the momentum equations over the VB control volume using the VB discretisation technique. The VB face velocity components are simply interpolated from nodal values using local linear interpolation functions:

$$(u_i)_f = \sum_{j=1}^{n} N_j (u_i)_j \tag{28}$$

where n is the number of nodes associated with the element that contains the face.

The pressure gradient term which enters the momentum equations as a source term is a little more difficult to evaluate. The assumption is made that the pressure gradient across a sub-control volume is approximately equal to the pressure gradient over the element containing the sub-volume. Any errors arising from this assumption would tend to zero as the mesh is refined. Using equation (7) to obtain the pressure gradient over an element leads to the element pressure gradient term being a function of alternate pressure values. Summing the element pressure gradients over the entire VB control volume:

$$\left(\frac{\partial p}{\partial x_i}\right)_{\mathrm{cv}} = \sum_{j=1}^{\mathrm{ne}} \left(\frac{\partial p}{\partial x_i}\right)_j \tag{29}$$

where ne is the number of elements of which the control volume node is a vertex. This results in the VB pressure gradient being a function of a series of adjacent pressure values. Unfortunately, due to cancelling out, a checkerboard pressure field would result in a zero pressure gradient across the VB control volume. A checkerboard pressure field is still perceived as a uniform pressure field by the momentum equations.

As with the VB procedure an element face velocity $\hat{\underline{u}}_{\mathrm{e}}$, dependent upon adjacent pressure values, needs to be defined. Nodal pseudo velocities $\hat{\underline{u}}_n$ are defined as equation (15) and nodal pressure gradient coefficients as:

$$d^{u_i} = a_{u_i}^{-1} \tag{30}$$

Since, each element face has a vertex located at its corner, element pseudo velocities and pressure gradient coefficients are simply averaged from corner values:

$$(\hat{u}_i)_{\mathrm{e}} = \frac{\sum_{j=1}^{n} (\hat{u}_i)_j}{n} \tag{31}$$

and:

$$\left(d_f^{u_i}\right)_{\mathrm{e}} = \frac{\sum_{j=1}^{n} d_j^{u_i}}{n} \tag{32}$$

where n is the number of element face corners.

An equation for the element face velocity $\tilde{\underline{u}}_{\mathrm{e}}$ may be defined as:

$$(\tilde{u}_i)_{\mathrm{e}} = (\hat{u}_i)_{\mathrm{e}} - \left(d_f^{u_i}\right)_{\mathrm{e}} (\nabla_{x_i} p)_f \tag{33}$$

where the pressure gradient across the element face is evaluated as:

$$(\nabla_{x_i} p)_f = A_f n_{x_i} (p_A - p_P) \tag{34}$$

Discretising the continuity equation (4) using the $\hat{\underline{u}}$ field and substituting in equation (33) leads to:

$$\sum_f \rho_f \frac{A_f^2 n_i^2}{a_i} (p_P - p_A)_f = \frac{\rho_P^0 V_P^0 - \rho_P V_P}{\Delta t} - \sum_f A_f \rho_f (\hat{\underline{u}} \cdot \underline{n})_f \tag{35}$$

where the subscript i in the first term indicates a summation over the three coordinate directions.

Again the pressure equation can be transformed into a pressure correction equation as (22). No relaxation is applied to pressure. Mass is conserved over the element and the momentum equations are used as a means of advancing the solution, a standard relaxation factor of 0.7 is applied to velocities. The nodal velocities are updated using equation (23).

5. Test case – lid-driven cavity

The co-located CC, co-located VB and hybrid solution methods, outlined in the previous paragraphs, are applied to the solution of flow only. Solutions are obtained on a Cartesian and distorted meshes with the same number of elements. The results are compared with benchmark solutions and a measure of the error due to mesh distortion is made. The aim is to validate the solution methods and test their ability to handle mesh skewness.

This case considers flow induced in a square cavity by moving the high y boundary wall. All of the other boundary walls are stationary. The initial velocity field was set to zero in the whole domain. The velocity on the moving boundary was set to $1\,\mathrm{m\,s^{-1}}$ in the x-direction. The pressure was fixed to zero in the centre of the cavity. Material properties were set to give a Reynolds number of 100, density $\rho = 1\,\mathrm{kg\,m^{-3}}$ and kinematic laminar viscosity $v_{\mathrm{lam}} = 0.01\,\mathrm{m^2\,s} > {}^{-1}$. A steady state solution was sought. The results obtained are compared against the solutions of Ghia *et al.* (1982) who produced a set of benchmark solutions using the multigrid technique and 99 elements in both the x- and y-direction. The CC and VB co-located techniques and the two hybrid discretisation methods are validated with the benchmark solutions using a Cartesian mesh of 99 by 99 elements. Results are compared with solutions obtained employing a much coarser mesh, 35 elements in both the x- and y-direction, with different degrees of skewness. Figures 3-5 show the meshes employed in the simulations, with mesh 1 being a standard Cartesian mesh, mesh 2 and 3 are distorted versions of mesh 1. The discretisation methods employed are:

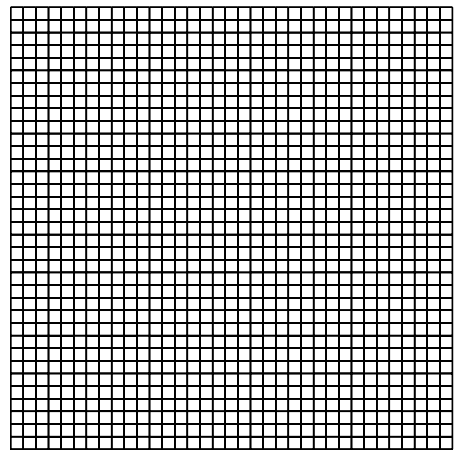

Figure 3.
Mesh 1

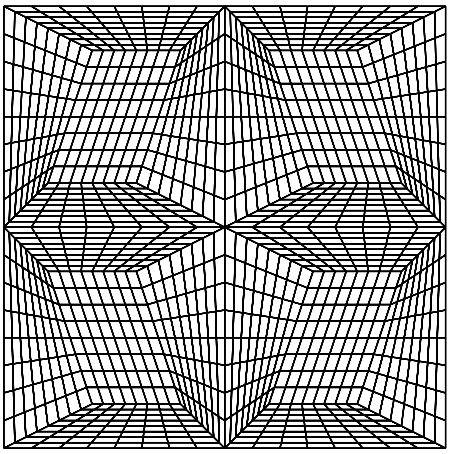

Figure 4.
Mesh 2

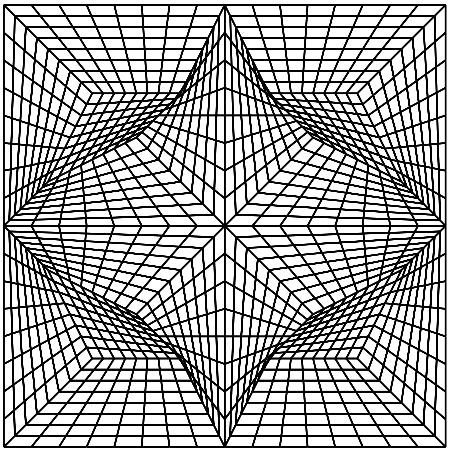

Figure 5.
Mesh 3

- velocity and pressure co-located at element centre (cc);
- velocity and pressure co-located at mesh vertex (vb);
- velocity solved at element centre and pressure at mesh vertex (ve pn); and
- velocity solved at mesh vertex and pressure at element centre (vn pe).

Velocity profiles are plotted for the u-velocity component, on a line parallel to the moving lid midway up the domain, and for the v-velocity component, perpendicular to the moving lid across the centre of the domain. For comparison purposes the velocity components are all plotted at the same geometric location, the mesh nodes, values being extrapolated from element values when velocity is solved at the element centre. This may lead to some extrapolation error in the boundary values of velocity components solved cell centred.

5.1 Results

Figure 6 shows the simulation results for a Cartesian 99 by 99 element mesh and the benchmark solutions of Ghia *et al.* (1982). As can be seen from Figure 6 all the solution methods are in good agreement with the benchmark solutions.

Figures 7-10 show the results obtained for simulations performed on meshes 1-3, where the mesh density, approximately 1,225 elements, is much reduced. Included for comparison purposes are the results obtained on the much finer 99 by 99 element Cartesian mesh. Mesh 1 tests the ability of the solution method to obtain results on a fairly coarse mesh. Meshes 2 and 3 test the ability of the methods to handle distortion in a mesh. For

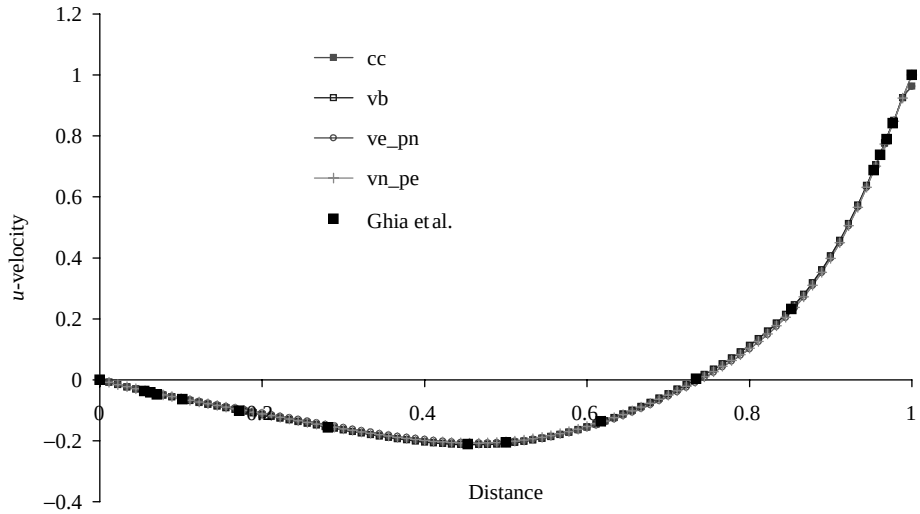

(a) *u*-velocity profiles

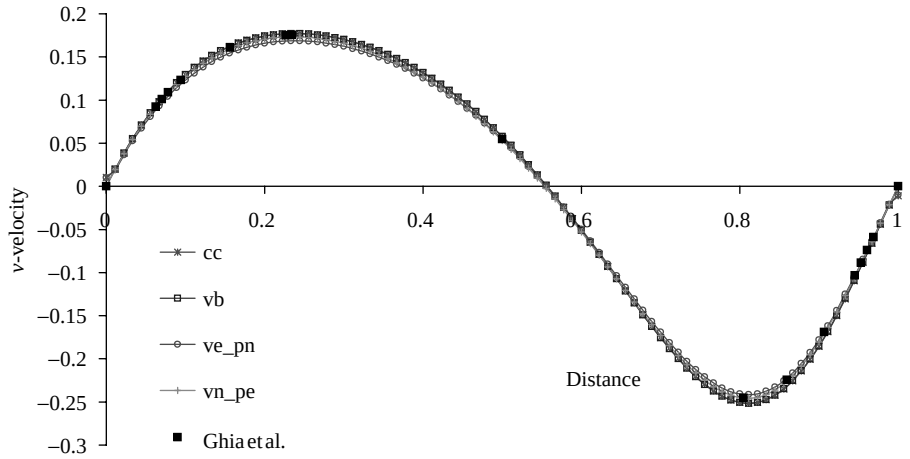

(b) *v*-velocity profiles

Figure 6.
Cartesian mesh 99 by 99 elements

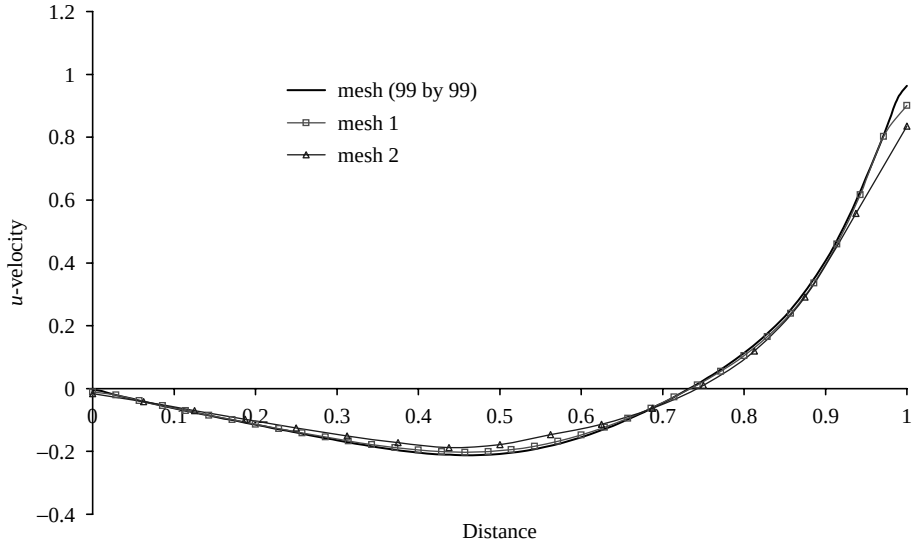

(a) *u*-velocity profiles

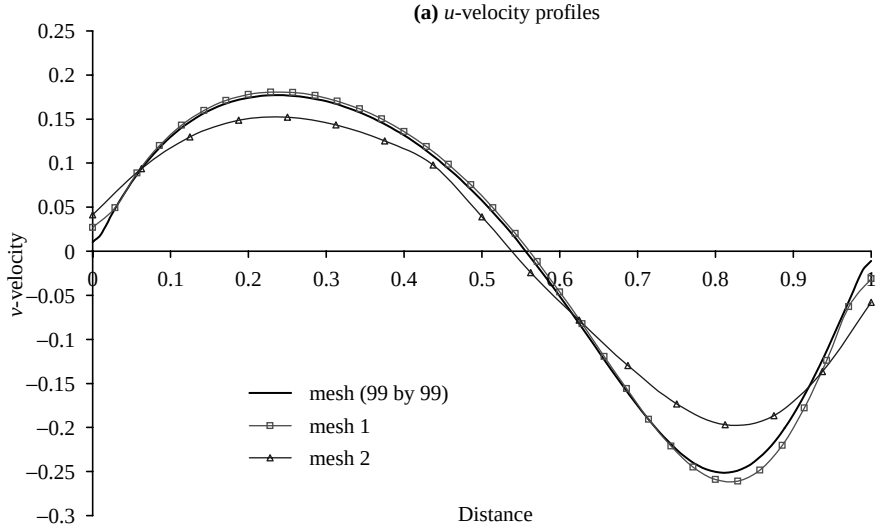

(b) *v*-velocity profiles

Figure 7.
Co-located CC method

both the distorted meshes 2 and 3, divergence was encountered if CC non-orthogonal correction terms were included. For this reason, the cc and ve pn methods discretise the momentum equations without the inclusion of these terms. The vb approach (Figure 8) handled all the meshes extremely well and good agreement was obtained with the solutions on the 99 by 99 element mesh. The cc results (Figure 7) failed to resolve the local minimum and maximum values of the *v*-velocity on mesh 2 and the solution failed on mesh 3 due to divergence. Convergence was achieved for the hybrid formulations on all meshes. The hybrid results seem dependent on the type of mesh employed, with no one method

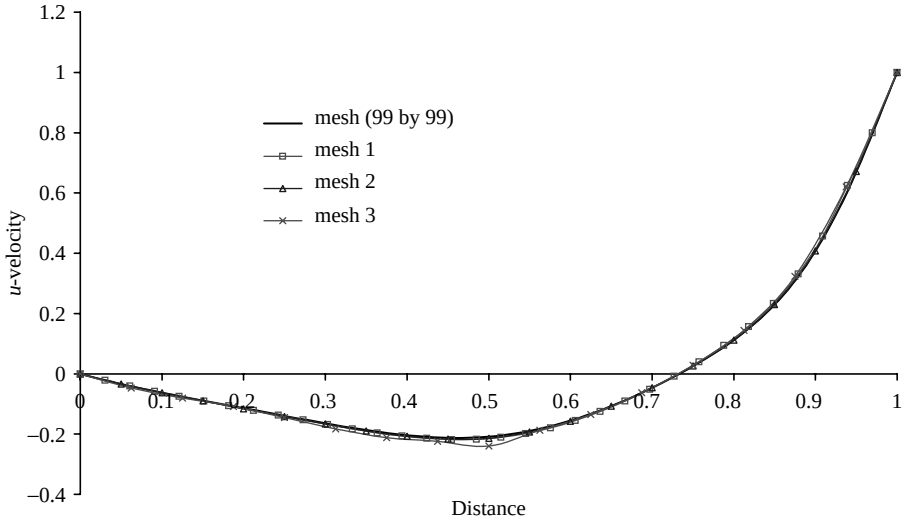

(a) *u*-velocity profiles

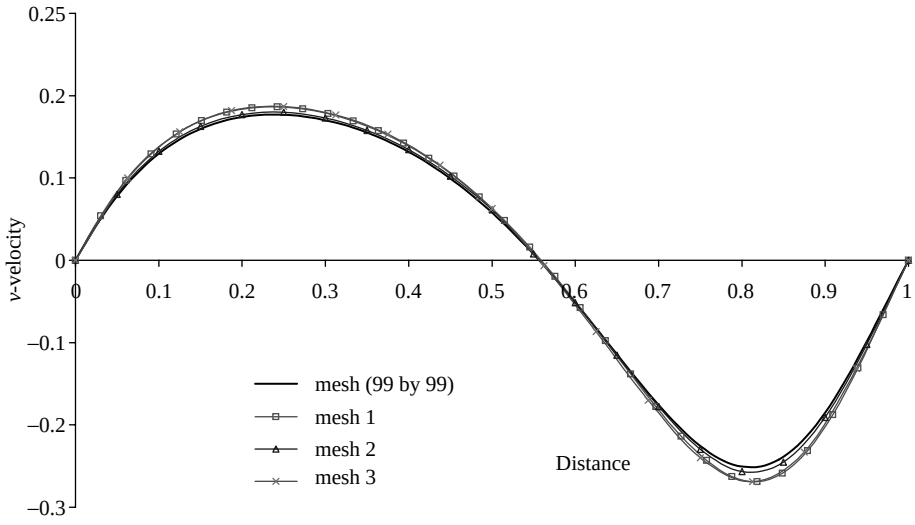

(b) *v*-velocityprofiles

Figure 8.
Co-located VB method

handling both distorted meshes well. Solving vn pe (Figure 10) gave reasonable results on mesh 2, the *u*-velocity profiles were in good agreement and the *v*-velocity profiles came close to achieving local maximum and minimum values. However, on mesh 3 the results degenerated and there were significant errors in both *u*- and *v*-velocity profiles. Conversely, using the ve pn formulation (Figure 9) the distortion in mesh 3 was handled well and only slight errors were obtained in the solution. Mesh 2 solutions for the *u*-velocity were reasonable but the *v*-velocity solutions completely failed to resolve the

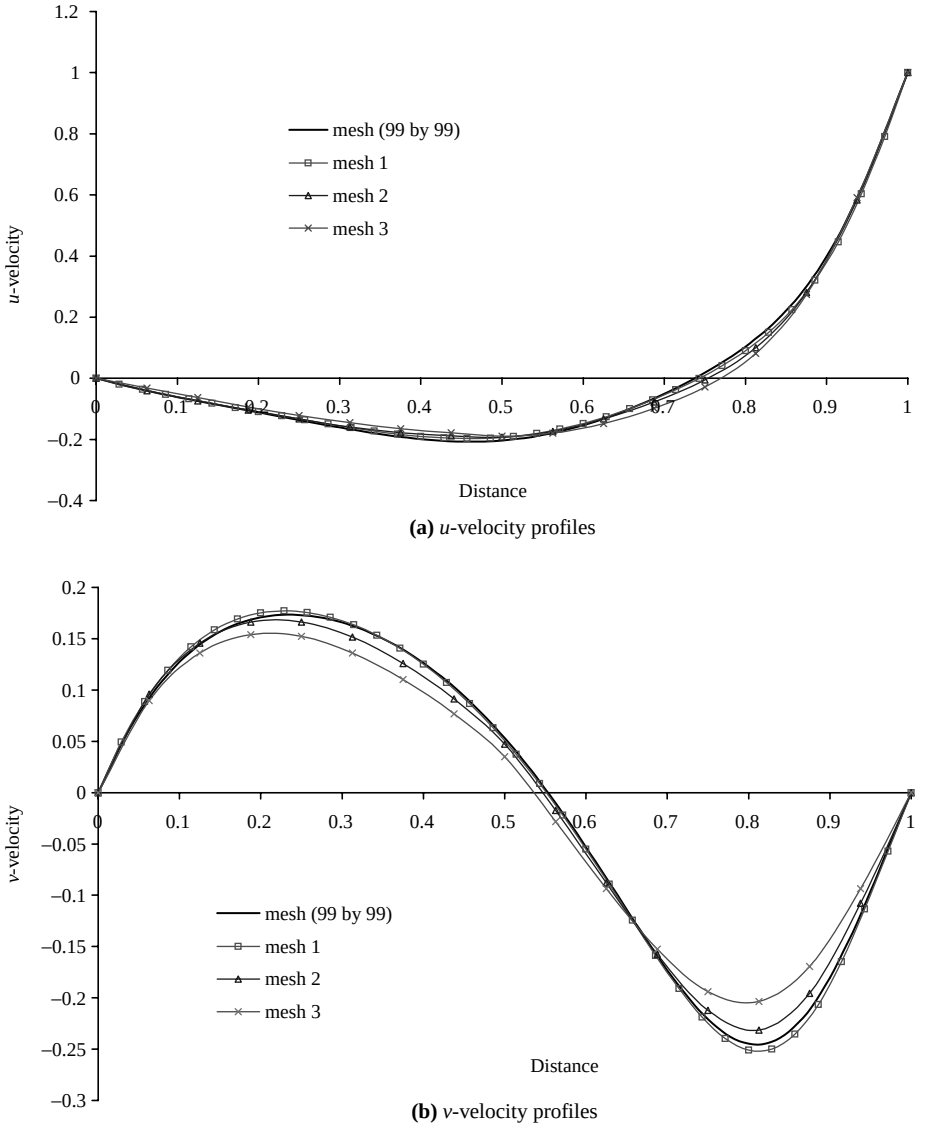

Figure 9.
Velocity solved CC, pressure solved VB, ve pn method

local maximum and minimum values. A measure of the error due to mesh distortion is given in Table I. The error was calculated using the VB solutions, obtained on the 99 by 99 mesh, as the base results and the error normalised using the value of the lid velocity.

5.2 Convergence behaviour and run times

The solutions were considered converged when the L_2 norm of the change in the solution of all the flow variables fell to 10^{-3}. The flow residuals were monitored during the solution procedure and the logarithm of the L_2 norm is shown as a function of the

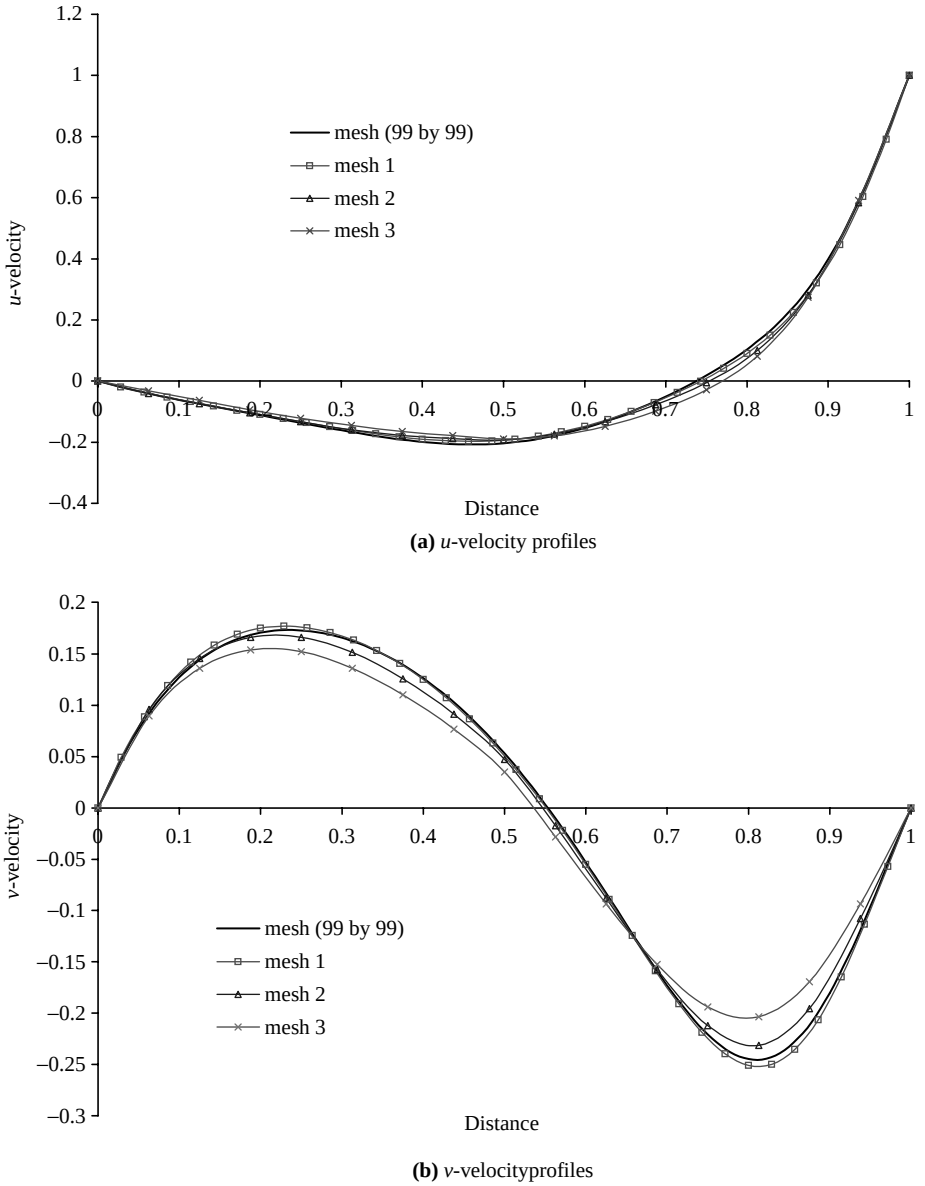

Figure 10.
Velocity solved VB, pressure solved CC, vn_pe method

number of iterations in Figures 11-14 for mesh 1. In the cc solution method (Figure 11) only slight oscillations occur in the pressure residuals and convergence was achieved in 112 iterations. Much larger oscillating pressure residuals are encountered when solving using the vb method (Figure 12). After approximately 90 iterations the pressure residual oscillations reduce and convergence is achieved in 129 iterations. In both methods only very slight oscillations occur in the velocity residuals. In the

	u-velocity (per cent)	*v*-velocity (per cent)
vb		
Mesh 2	0.15	0.26
Mesh 3	0.88	0.66
cc		
Mesh 2	2.96	3.00
Mesh 3	–	–
ve_pn		
Mesh 2	4.63	3.72
Mesh 3	3.02	2.46
vn_pe		
Mesh 2	1.57	1.46
Mesh 3	3.05	3.18

Table I.
Normalised error due to mesh distortion 24

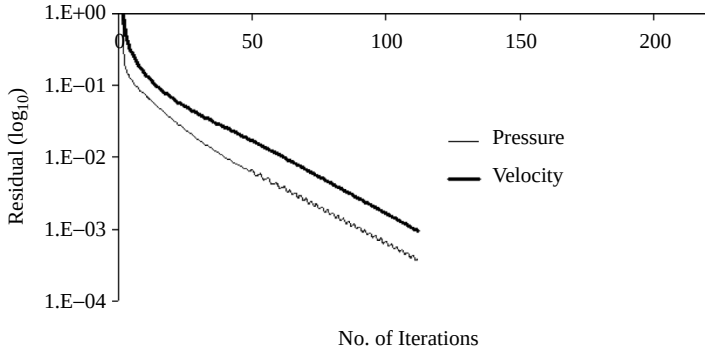

Figure 11.
Co-located CC: solution residual history vs iterations

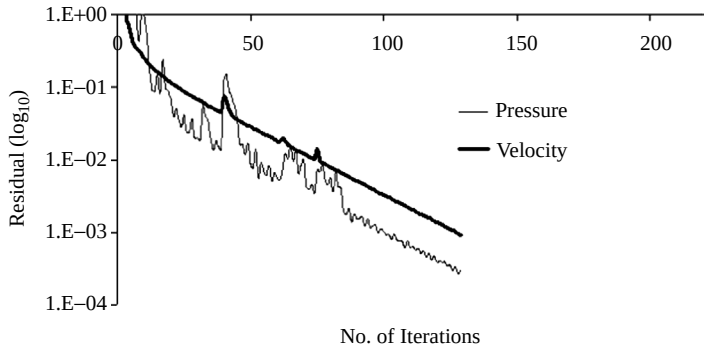

Figure 12.
Co-located VB: solution residual history vs iterations

ve_pn solution method (Figure 13) only slight oscillations are encountered in the residuals but convergence is slow requiring 216 iterations. The vn_pe solution method (Figure 14) produces large oscillations in the pressure and *u*-velocity residuals but convergence is achieved in 113 iterations.

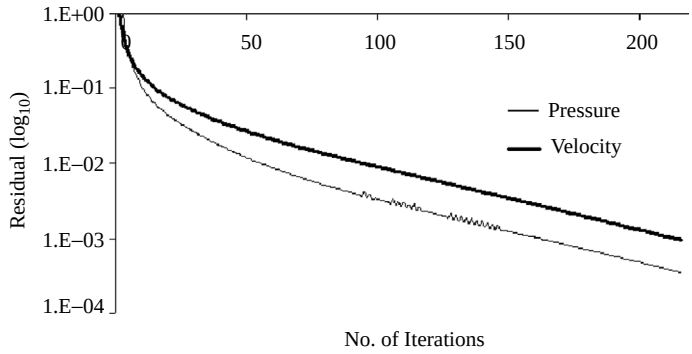

Figure 13.
Velocity CC, pressure VB (ve_pn): solution residual history vs iterations

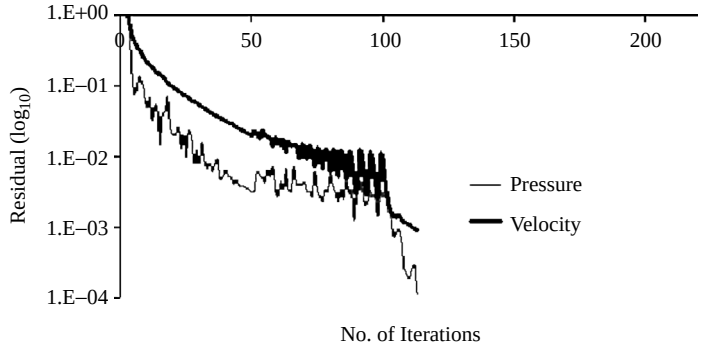

Figure 14.
Velocity VB, pressure CC (vn_pe): solution residual history vs iterations

The moving lid cavity case is a 2D problem but simulations were carried out on a mesh of hexahedral elements. In this case, there are over twice as many mesh vertices than elements. Solving VB, variables are resolved in 2D planes. Hence, in order to compare the solution methods, run times are given as an average per variable per solution point and are shown in Table II for all the meshes investigated. The simulations were performed on an AMD Athlon 1.39 GHz processor. The run times are case and mesh dependent, for the Cartesian mesh, the vb method took approximately 4.5 times the cc method. Of the hybrid methods solving vn pe was the fastest taking approximately 2.5 times longer than cc. The ve pn method was very slow to converge, the number of iteration required to achieve convergence was approximately 1.6-1.9 times the other methods. As a result the run time per variable per solution point was eight times

Table II.
Run times per variable per solution point

	Mesh 1	Mesh 2	Mesh 3
cc	5.44×10^{-4}	5.44×10^{-4}	–
vb	2.44×10^{-3}	4.88×10^{-3}	5.53×10^{-3}
ve_pn	4.36×10^{-3}	7.93×10^{-3}	7.33×10^{-3}
vn_pe	1.4×10^{-3}	2.65×10^{-3}	2.5×10^{-3}

greater than the cc technique. The cc run time remained constant for meshes 1 and 2. The vb and hybrid run times increased when solving on the distorted meshes 2 and 3.

The memory requirements for VB solutions are far greater than CC solutions. Storing the geometric requirements for a VB control volume requires approximately 590 bytes compared to only 179 bytes for a CC control volume. Extra memory is also required in the solution of a VB variable. For the solution of the moving lid problem on meshes comprising of 8,100 elements and 16,562 vertices the average memory requirements per solution point was as follows: cc – 92 bytes, vb – 245 bytes, ve_pn – 381 bytes and vn_pe – 336 bytes.

5.3 Discussion

The cavity flow problem illustrates the ability of the co-located VB method to handle mesh distortion. There is no significant difference in the simulation results obtained on the distorted meshes compared to those on the standard Cartesian mesh. Conversely, the co-located CC method struggles to produce solutions on the distorted mesh and the solution diverges on mesh 3. The inclusion of non-orthogonal correction terms, in an effort to improve the CC solutions, can introduce more instabilities into the solution process. The CC results can be significantly improved on meshes where the inclusion of correction terms produce solutions. However, on severely distorted meshes erroneous or diverging results are often encountered.

The hybrid schemes did enable solutions on all the meshes, however, the solutions obtained on the distorted meshes included non-orthogonal errors of varying degrees. Solving the pressure VB allows for pressure gradients to be more accurately represented on the distorted meshes, the VB method (equation (19)) calculates the face pressure gradient from eight vertex values for a hexahedral element whereas the CC method (equation (34)) calculates face gradients from only two adjacent element values. However, the CC discretisation of the momentum equations still contain non-orthogonal errors. These errors are then passed into the pressure equation via the pseudo-velocities. The velocity components are updated from the pseudo-velocities and VB pressure gradients. Improving the resolution of the pressure field on a non-orthogonal mesh directly influences the velocity components, but non-orthogonal errors in the discretised momentum equations still pass into the final solution. The critical region in the cavity flow problem for recirculating flow is the mesh quality in the top right hand corner. Although mesh 3 is overall the most distorted, in the critical region mesh 2 is more non-orthogonal. The non-orthogonal errors in the discretised CC momentum equations in this region result in a weaker recirculation of flow on mesh 2. Solving the momentum equations VB allows good resolution of pseudo-velocities to be obtained on the distorted meshes but the discretised CC pressure equation will still include non-orthogonal errors. These errors in the pressure field will pass into the momentum equations through the pressure gradient term. In the cavity flow problem the errors in the pressure field result in a weaker recirculation of flow as the mesh became more distorted.

6. Conclusion

It is now well established that the CC discretisation technique produces expeditious and reliable solutions of the Navier-Stokes flow equations on orthogonal meshes. For problems, where the geometry can be represented by a good quality mesh the CC method is computationally efficient producing a diagonally dominant solution matrix

that can be solved speedily by nearly any iterative solve. However, fitting a highly orthogonal mesh to a complex geometry can be one of the most time consuming aspects of the modelling process. On distorted meshes the inclusion of non-orthogonal correction terms during the discretisation process to account for non-orthogonality in the mesh can be problematic. On arbitrarily distorted meshes divergence is often encountered. Solving without accounting for mesh non-orthogonality introduces inaccuracies, with solutions having some dependence on the mesh skewness. When convergence is obtained on highly distorted meshes the solutions are often highly inaccurate. The non-orthogonal errors introduced into the solution method are multiplied when solving coupled variables. For flow solutions, errors in the velocity field will effect pressure solutions and vice versa. In this way errors accumulate, increasing as the solution procedure progresses. For multi-physics multi-mesh problems, such as coupled flow and stress problems, mesh deformation can occur during the solution procedure introducing non-orthogonality issues, see Slone *et al.* (2004) for a discussion of this challenge.

The VB discretisation technique has been shown to handle distorted meshes with ease. Solutions obtained on skewed meshes are comparable with solutions obtained on a uniform Cartesian mesh. The computational requirements of the VB discretisation method are its main drawback. On a stationary mesh the discretisation procedure can be accelerated by the storage of the elemental shape functions and their derivatives at local integration points. However, on a moving mesh these quantities, which require the inversion of a Jacobian matrix associated with each element, need to be recalculated at each time-step. This plus the additional topological and control volume specifications makes the VB technique computationally very expensive. The VB solution matrix is symmetric for sub-control volumes of equal size or asymmetric for unequal sub-control volumes, and positive-definite with a much larger bandwidth than the solution matrix of the CC discretisation procedure. The increased communication between solution points leads to less solver iterations required to obtain solutions but increased solver computational time. Solving directly on the boundary wall, boundary solutions are more accurately represented and boundary information is more readily passed through the solution domain. The VB computational time, per solved variable, is approximately 1.8 times that of the CC method. The additional time requirements can be offset by time saved in mesh generation. But the solution of additional variables increasingly adds to the VB simulation time.

In an attempt to reduce computational requirements, whilst retaining the ability of the VB technique to handle mesh distortion, hybrid flow solutions were investigated. The partially staggered hybrid formulations and co-located techniques investigated require specialist discretisation techniques to avoid checkerboard pressure predictions. Discretising either the momentum or continuity equation using VB techniques allowed the solution on distorted meshes where purely CC techniques fail. However, non-orthogonal errors introduced through CC discretisation degraded the solutions and results appear to have some dependence on the distorted mesh. Discretising the momentum equations using VB methods allows better solution of vertex velocity components, but face velocity components are dependent on CC face pressure gradients. Errors in defining the pressure gradient across the face of a distorted control volume are introduced into the solution process. Solving pressure using VB discretisation allows for face pressure gradients to be more accurately represented, but

non-orthogonal errors are still included in the CC discretisation of the momentum equations. Neither of the hybrid formulations gave consistently better results on all meshes investigated.

In summary, the VB discretisation technique for the solution of flow gave comparable solutions on all meshes investigated but is computationally expensive and requires considerable software restructuring for existing CFD software tools. A novel discretisation approach will be outlined in a following paper (McBride *et al.*, *in preparation*), this method utilises the VB approach for the flow solution and employs well established physics models that use CC techniques for other transported properties. This combined VB – CC approach, allows solutions on highly distorted meshes that defeat purely CC solutions and is relatively straightforward to embed within generic CC based CFD tools.

References

Ammara, I. and Masson, C. (2004), "Development of a fully coupled control-volume finite element method for the incompressible Navier-Stokes equations", *Int. J. Num. Meth. in Fluids*, Vol. 44, pp. 621-44.

Baliga, B.R. (1996), *Advances in Numerical Heat Transfer*,Vol. 1, Hemisphere Publishing Corporation, Washington, DC.

Barth, T.J. (1992), "Aspects of unstructured grids and finite-volume solvers for the Euler and Navier-Stokes equations", AGARD Report,Vol. 787, pp. 61-661.

Barth, T.J. and Jespersen, D.C. (1989), "The design and application of upwind schemes on unstructured meshes", AIAA Paper, 89-0366.

Bijl, H., van Zuijlen, A.H. and van Mameren, P. (2005), "Validation of adaptive unstructured hexahedral mesh computations of flow around a wind turbine airfoil", *Int. J. Num. Meth. Fluids*, Vol. 48 No. 9, pp. 929-45.

Boivin, S., Cayre, F. and Herard, J.M. (2000), "A finite volume method to solve the Navier-Stokes equations for incompressible flows on unstructured meshes", *Int. J. Therm. Sci.*, Vol. 39, pp. 806-25.

Braaten, M. and Shyy, W. (1986), "A study of recirculating flow computation using boundary-fitted co-ordinates: consistency aspects and mesh skewness", *Num. Heat Transfer*, Vol. 9, pp. 559-74.

Burns, A.D. and Wikkles, N.S. (1987), *A Finite Difference Method for the Computation of Fluid Flows in Complex Three Dimensional Geometries*, AERE R 12342, Harwell Laboratory, Oxfordshire, UK.

Chakrabartty, S.K. (1990), "Vertex-based finite-volume solution of the two-dimensional Navier-Stokes equations", *AIAA J.*, Vol. 28 No. 10, pp. 1829-31.

Chan, A.J. and Kallinderis, Y. (1998), "Adaptive hybrid (prismatic-tetrahedral) grids for incompressible flows", *Int. J. Num. Meth. Fluids*, Vol. 26, pp. 1085-105.

Chand, K.K. (2005), "Component-based hybrid mesh generation", *Int. J. Num. Meth. Engineering*, Vol. 62 No. 6, pp. 747-33.

Chavent, G., Younes, A. and Ackerer, P. (2003), "On the finite volume reformulation of the mixed finite element method for elliptic and parbolic PDE on triangles", *Comput. Meth. Appl. Mech. Engrg*, Vol. 192, pp. 655-82.

Cho, M.J. and Chung, M.K. (1994), "New treatment of nonorthogonal terms in the pressure correction equation", *Num. Heat Transfer, Part B*, Vol. 26, pp. 133-45.

Coirier, W.J. (1994), "An adapitiely-refined, cartesian, cell-based scheme for the Euler and Navier-Stokes equations", NASA TM-106754.

Croft, T.N. (1998), "Unstructured mesh – finite volume algorithms for swirling, turbulent, reacting flows", PhD thesis, The University of Greenwich, London.

Croft, N., Pericleous, K.A. and Cross, M. (1995), "PHYSICA: a multiphysics environment for complex flow processes", in Taylor, C. and Durbetaki, P. (Eds), *Numerical Methods in Laminar and Turbulent Flow '95*,Vol. 2, pp. 1269-80.

Crumpton, P.I. and Giles, M.B. (1995), "Aircraft computations using multigrid and unstructured parallel library", AIAA, 95-0210.

Demirdzic, I. (1982), "A finite volume method for the computation of fluid flow in complex geometries", PhD thesis, University of London, London.

Dervieux, A. (1985), "Steady Euler simulations using unstructured meshes", VKI Lect. Ser., 1884-04.

Durlofsky, L.J. (1993), "A triangle based mixed finite-element-finite volume technique for modelling two phase flow through porous media", *J. Comp. Physics*, Vol. 105, pp. 252-66.

Ghia, U., Ghia, K.N. and Shin, C.T. (1982), "High-re solutions for incompressible flow using the Navier-Stokes equations and a multigrid method", *J. Computational Physics*, Vol. 48, pp. 387-411.

Hallo, L., Le Ribault, C. and Buffat, M. (1997), "An implicit mixed finite-volume-finite-element method for solving 3D turbulent compressible flows", *Int. J. Num. Meth. Fluids*, Vol. 25, pp. 1241-61.

Haselbacher, A. and Blasek, J. (2000), "On the accurate and efficient discretization of the Navier-Stokes equations on mixed grids", *AIAA J.*, Vol. 38, pp. 2094-102.

Hsu, C. (1981), "A curvilinear-coordinate method for momentum, heat and mass transfer in domains of irregular geometry", PhD thesis, University of Minnesota, Minneapolis, MN.

Jameson, A., Baker, T.J. and Weatherill, N.P. (1986), "Calculation of inviscid transonic flow over a complete aircraft", AIAA, 86-0103.

Koobus, B. and Farhat, C. (2004), "A variational multiscale method for the large eddy simulation of compressible turbulent flows on unstructured meshes – application to vortex shedding", *Comput. Meth. Appl. Mech. Engrg*, Vol. 193, pp. 1367-83.

Lehnhauser, T. and Schafer, M. (2002), "Improved linear interpolation practice for finite-volume schemes on complex grids", *Int. J. Num. Meth. Fluids*, Vol. 38, pp. 625-45.

Lehnhauser, T. and Schafer, M. (2003), "Efficient discretisation of pressure-correction equations on non-orthogonal grids", *Int. J. Num. Meth. Fluids*, Vol. 42, pp. 211-31.

Lyra, P.R.M., Morgan, K., Peraire, J. and Peiro, J. (1994), "TVD algorithms for the solution of the compressible Euler equations on unstructured meshes", *Int. J. Num. Meth. Fluids*, Vol. 19, pp. 827-47.

McBride, D. (2003), "Vertex-based discretisation methods for thermo – fluid flow in a finite volume – unstructured mesh context", PhD thesis, The University of Greenwich, London.

McBride, D., Croft, T.N. and Cross, M. (n.d.), "A coupled finite volume method for the solution of flow problems on complex geometries", *Int. J. Num. Meth. Fluids* in press, Published online 2006; DOI 10.1002/fld.1250.

Mavriplis, D.J. (1995), "Three-dimensional multigrid Reynolds-averaged Navier-Stokes solver unstructured meshes", *AIAA J.*, Vol. 33, pp. 445-53.

Mazzia, A. and Putti, M. (2005), "High order Godunov mixed methods on tetrahedral meshes for density driven flow simulations in porous media", *J. Comp. Physics*, Vol. 208, pp. 154-74.

Moulinec, C. and Wesseling, P. (2000), "Colocated schemes for the incompressible Navier-Stokes equations on non-smooth grids for two-dimensional problems", *Int. J. Num. Meth. Fluids*, Vol. 32, pp. 349-64.

Patankar, S.V. and Spalding, D.B. (1972), "A calculation procedure for heat, mass and momentum transfer in three-dimensional parabolic flows", *International Journal of Heat and Mass Transfer*, Vol. 15, pp. 1787-806.

Peric, M. (1985), "A finite volume method for the prediction of three-dimensional fluid flow in complex ducts", PhD thesis, University of London, London.

Peric, M. (1990), "Analysis of pressure-velocity coupling on nonorthogonal grids", *Num. Heat Transfer, Part B*, Vol. 17, pp. 63-82.

Perron, S., Boivin, S. and Herard, J-M. (2004), "A new finite volume discretisation scheme to solve 3D incompressible thermal flows on unstructured meshes", *Int. J. Therm. Sci.*, Vol. 43, pp. 833-48.

Prakash, C. and Patankar, S.V. (1985), "A control volume-based finite-element method for solving the Navier-Stokes equations using equal-order velocity-pressure interpolation", *Numerical Heat Transfer*, Vol. 8, pp. 259-80.

Reyes, M., Rincon, J. and Damia, J. (2001), "Simulation of turbulent flow in irregular geometries using a control-volume finite-element method", *Numerical Heat Transfer, B*, Vol. 39, pp. 79-89.

Rhie, C.M. and Chow, W.L. (1983), "Numerical study of the turbulent flow past an aerofoil with trailing edge separation", *AIAA J.*, Vol. 21 No. 11, pp. 1525-32.

Slone, A.K., Pericleous, K., Bailey, C., Cross, M. and Bennett, C. (2004), "A finite volume unstructured mesh approach to dynamic fluid-structure interaction: an assessment of the challenge of predicting the onset of flutter", *Appl Math. Modelling*, Vol. 28, pp. 211-39.

Sorensen, K.A., Hassan, O., Morgan, K. and Weatherill, N.P. (1999), *An Aglomeration Unstructured Hybrid Mesh Mehtod for 2D Turbulent Compressible Flows*, ISCFD, Bremen.

Taylor, G.A., Bailey, C. and Cross, M. (2003), "A vertex-based finite volume method applied to non-linear material problems in computational solid mechanics", *International Journal for Numerical Methods in Engineering*, Vol. 56, pp. 507-29.

Wapperom, P. and Webster, M.F. (1998), "A second-order hybrid finite-element volume method for viscoelastic flows", *J. Non-Newtonian Fluid Mech.*, Vol. 79 Nos 2/3, pp. 405-31.

Weiss, J.M., Maruszewski, J.P. and Smith, W.A. (1999), "Implicit solution of preconditioned Navier-Stokes equations using algebraic multigrid", *AAIA J.*, Vol. 37 No. 1, pp. 29-36.

Zhu, M., Shimizu, Y. and Nishimoto, N. (2004), "Calculation of curved open channel flow using physical curvilinear non-orthogonal co-ordinates", *Int. J. Num. Meth. Fluids*, Vol. 44, pp. 55-70.

Zienkiewicz, O.C. and Morgan, K. (1983), *Finite Element and Approximation*, Wiley, New York, NY.

Further reading

Barth, T.J. (1993), "Recent developments in high order k-exact reconstruction on unstructured meshes", AIAA, 93-0668.

Corresponding author

D. McBride can be contacted at: d.mcbride@swan.ac.uk